

Improvement of Battery State of Charge Estimation Using Recursive Least Squares-Based Adaptive Extended Kalman Filter

Ramazan Havangi¹ | Fatemeh Karimi²

Faculty of Electrical Engineering and Computer, University of Birjand, Birjand, Iran.^{1,2}
Corresponding author's email: Havangi@Birjand.ac.ir

Article Info	ABSTRACT
<p>Article type: Research Article</p> <p>Article history: Received: 30-January-2024 Received in revised form: 26-March-2024 Accepted: 15-April-2024 Published online: 21-June-2024</p> <p>Keywords: Battery charge, State of the Charge (SOC), Kalman Filter, Estimation.</p>	<p>This paper presents an advanced methodology for SOC estimation by integrating Recursive Least Squares (RLS) techniques with Adaptive Extended Kalman Filter (AEKF). The proposed methodology aims to mitigate the challenges associated with fluctuating battery parameters and varying noise characteristics over time, which can significantly impact the accuracy of SOC estimation. By dynamically adjusting to evolving system dynamics and noise statistics, the proposed approach exhibits enhanced robustness and accuracy compared to traditional techniques. The proposed methodology assumes that battery parameters, including internal resistance, capacitance, and noise information, undergo variations over time. To address this assumption, two distinct online identification algorithms for parameters and noise information are introduced. Specifically, the RLS algorithm is utilized to ascertain resistance and capacitance values. Process and measurement noise covariance is also estimated based on an iterative noise information identification algorithm. Subsequently, all updated values are incorporated into the EKF. The results demonstrate that the RLS-AEKF approach achieves higher accuracy than the EKF. The results based on Fast Urban Driving Schedule (FUDS) and Urban Dynamometer Driving Schedule (UDDS) working current profiles validate the effectiveness of the proposed approach in enhancing SOC estimation accuracy under realistic operating conditions.</p>

I. Introduction

The global community is confronted with substantial environmental challenges, notably greenhouse gas emissions and global warming, which stem predominantly from the widespread utilization of petrol and diesel in vehicular operations. These fossil fuels are major contributors to the annual CO₂ emissions [1, 2]. In response to this pressing issue, electric vehicles (EVs) have emerged as a promising solution to mitigate carbon emissions, garnering significant attention amid the prevailing energy crisis [3, 4]. Batteries, renowned for their comparatively high energy density, low noise emissions, and minimal maintenance demands, have garnered widespread utilization in electricity storage technologies on both small and medium scales [5, 6]. Among various battery types, lithium-ion batteries are extensively employed in diverse EV applications. Given the paramount

importance of ensuring the safe and dependable operation of lithium-ion batteries, implementing a battery management system (BMS) is indispensable [6, 7].

Battery management technologies encompass a variety of estimations, including the assessment of parameters such as the state of charge (SOC), state of temperature (SOT), state of energy (SOE), state of power (SOP), state of health (SOH), and state of safety (SOS), among which SOC holds pivotal significance. SOC represents the proportion of a battery's remaining charge to its designated capacity. Precise anticipation of battery SOC serves as a preventive measure against both overcharging and over-discharging, thereby contributing to the overall extension of the battery's operational lifespan [1, 2].

Current prevalent methods for estimating SOC include the ampere-hour integration method, open circuit voltage

(OCV) method, data-driven method, and model-based method [1]. The ampere-hour integration method encounters challenges in accurately determining the initial SOC, and errors in current measurements exacerbate cumulative errors post-integration [8, 9]. The OCV method necessitates an extended resting period for obtaining the open circuit voltage, rendering it unsuitable for real-time SOC estimation [10, 11]. The data-driven method has garnered considerable attention for its adaptability and model-free advantages [11, 12]. However, this method relies heavily on the accuracy of training data, and it cannot guarantee precise SOC estimation under complex and unknown operational conditions [6, 7]. Artificial neural networks and fuzzy logic are the commonly employed data-driven methods [14, 15].

Unlike alternative approaches, model-based estimation methods offer enhanced robustness and accuracy, remaining unaffected by initial values and exhibiting lower computational overheads, rendering them well-suited for engineering applications [16]. The model-based approach requires the establishment of a battery model. Among model-based methods, the extended Kalman filter (EKF) is widely recognized as the most popular technique for estimating the SOC of batteries [17]. The EKF, introduced to enhance the performance of the linear Kalman filter through Taylor-series expansion, has been extensively utilized [17].

Different variants of the EKF are utilized for SOC estimation. For example, the dual-mode EKF is applied in [19, 20] to address aging phenomena. Additionally, adaptive EKF is employed in [21-23] to achieve rapid transient response.

Investigations into the SOC estimation show a close interdependence between the estimation accuracy and the values of the model parameters. It motivates the literature to propose a new method known as adaptive estimation. For instance, the problem of SOC estimation in the presence of the model uncertainty is discussed in [24], in which the authors have tried to solve the problem from both robust and adaptive estimation viewpoints. Similarly, in [25], the variation of the system parameters is considered in the adaptive EKF (AEKF) algorithm.

Although the literature commonly combines EKF and recursive least squares (RLS) methods, none have integrated noise information estimation within this framework. For example, [26] focuses on SOC estimation for EVs by employing a combination of RLS and nonlinear EKF. Their study emphasizes the importance of accurately updating battery parameters, particularly amidst fluctuating temperature and SOC conditions, to enhance SOC estimation precision. Similarly, [21] investigates SOC estimation for power batteries in unmanned aerial vehicles (UAVs),

highlighting the significance of lithium-ion batteries in UAV development and the need for precise SOC estimation to optimize flight performance. They propose a joint estimation algorithm utilizing a second-order resistor-capacitor (RC) network equivalent circuit model and an EKF for SOC estimation. Additionally, [27] addresses SOC estimation for hybrid vehicles, proposing an adaptive forgetting factor regression least-squares–extended Kalman filter (AFFRLS–EKF) strategy to improve accuracy amid changing charge and discharge conditions. While these studies offer valuable insights into SOC estimation, our research in this paper advances these methodologies by incorporating noise information estimation into the SOC estimation framework, thereby enhancing the accuracy and robustness of our approach.

The literature review shows that a gap still exists in the adaptive estimation of SOC in the presence of the model uncertainty. To provide more detail, the literature does not use parallel filters for SOC estimation when dealing with model uncertainty. To do this, the RLS-AEKF method presented in this paper integrates the principles of RLS and EKF to estimate the SOC of batteries. Unlike conventional EKF approaches, which rely on fixed process and measurement noise covariance matrices, RLS-AEKF adaptively adjusts these covariance matrices based on real-time data and system dynamics. This adaptive mechanism enables the RLS-AEKF algorithm to effectively handle uncertainties and variations in battery behavior, resulting in improved estimation accuracy and robustness. RLS-AEKF dynamically adjusts the process and measurement noise covariance matrices based on the evolving system dynamics and measurement uncertainties. This adaptive mechanism enhances the algorithm's resilience to changing operating conditions and improves estimation accuracy. Experimental studies and simulation results have demonstrated the robust performance of RLS-AEKF across various operating conditions. In summary, the superiority of the proposed method over other approaches is demonstrated in Table 1.

The paper is structured as follows. Section II provides the mathematical background of the system, including the battery equivalent model and relevant definitions. Section III discusses the fundamental concepts of the EKF design procedure. The adaptive SOC estimation is detailed in Section IV, where system identification and adaptive SOC estimation algorithms are presented. Section V examines the results to validate the proposed method. Finally, Section VI concludes the paper.

TABLE 1 ADVANTAGE OF THE PROPOSED METHOD

The proposed method	Other works
Introducing two distinct online identification algorithms for parameter and noise information: recursive least squares for determining resistance and capacitor values and an iterative method for estimating noise covariance	Utilizing existing methods without mentioning online identification algorithms for parameter and noise information.
Handling varying battery parameters and noise information over time to enhance SOC estimation accuracy	Specifically not addressing the challenge of handling time-varying battery parameters and noise information
Demonstrating improvement in SOC estimation accuracy by addressing uncertainties in model parameters and noise information through the proposed algorithms	It may not clearly show improvement in SOC estimation accuracy due to not addressing uncertainty in model parameters and noise information.

II. Mathematical Background

In model-based estimation, the model's accuracy leads to an accurate estimation, which is related to the dependence of the estimators on the model. Therefore, the first step in SOC estimation is to use a more accurate model. Different models have been addressed in the literature from the system identification point of view. For example, different models are explained in [1], where the main difference is to use a series of RC filters in the equivalent circuit.

Based on the literature, a common model of the battery is considered to be as shown in Fig. 1. The proposed method is in fact an equivalent model of a battery when driving a load. As can be seen, the battery is modeled as a DC voltage source connected to an RC filter and series resistance. Based on the equivalent circuit, the battery terminal voltage is achieved when the open circuit voltage passes through a filter. In a more accurate view, it can be seen that getting more power from the battery (at a constant voltage) leads to more loss in power when passing through the series filter. The mathematical model of the battery can be divided into two parts: an SOC model and an equivalent circuit model. This subsection presents these models separately, and then the final model is produced by integrating them.

A. Battery SOC definition

A battery's SOC is defined as the ratio of the available capacity to the maximum potential capacity that it can supply. The mathematical representation of SOC is as follows:

$$SOC(t) = SOC(t_0) - \frac{\eta}{C_n} \int_{t_0}^t I(t) dt \quad (1)$$

where $SOC(t_0)$ and $SOC(t)$ represent SOC at initial time t and at time t_0 , respectively, η represents the coulombic efficiency, which signifies the ratio of the battery discharge capacity to the charge capacity during the same cycle. Also, C_n is the battery's total capacitor and $I(t)$ shows its terminal current. Note that in Eq. (1), the positive sign is used for the battery charging, and correspondingly, the negative sign is used for the discharging. A discrete representation of (1) is as follows:

$$SOC(k) = SOC(k-1) - \frac{\eta I(k) T_s}{C_n}$$

where T_s denotes the sampling interval and $I(k)$ signifies the current load. $SOC(k)$ and $SOC(k-1)$ denote the battery's SOC at time step k and $k-1$, respectively.

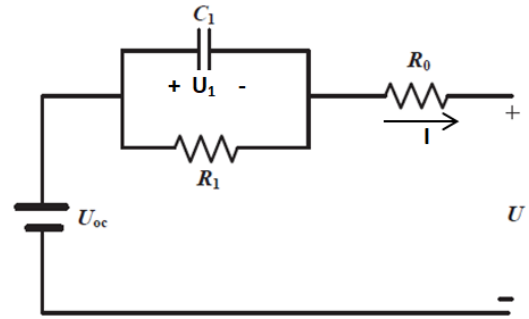


Fig. 1. Equivalent circuit of the battery

B. Battery Dynamical Model

To write the dynamical model of the battery, researchers have used the basic Kirshof laws to write the dynamical model. In more detail, note that in Fig.1, U_{oc} depicts the OCV. Also, U is the terminal voltage of the battery and the inner capacity and resistance is shown with C_1 and R_1 , respectively. Therefore, the mathematical model of the battery can be written as:

$$U = U_{oc} - R_0 I - U_1$$

$$\frac{dU_1}{dt} = \frac{-U_1}{R_1 C_1} + \frac{I}{C_1} \quad (2)$$

in which U_1 is the voltage of the RC circuit. In addition, the total current of the battery is shown by I . The battery voltage can be written with the solution of the second differential equation as:

$$U_1(k) = U_1(k-1) e^{-\frac{T_s}{R_1 C_1}} + R_1 I(k) (1 - e^{-\frac{T_s}{R_1 C_1}}) \quad (3)$$

in which $I(k)$ is the value of the total current in the sample of k . Similarly, the notations $U_1(k)$ and $U_1(k-1)$

shows the voltage of the RC circuit in the sampling time of k and $k-1$, respectively. If the current and voltage with the related parameters of the above equations are known, then the OCV can be written as:

$$U_{OC}(k) = U(k) + I(k)R_o + U_1(k-1)e^{-\frac{T_s}{R_1C_1}} + R_1I(k)(1 - e^{-\frac{T_s}{R_1C_1}}) \quad (4)$$

Note that Eq. 3 and 4 can be described as:

$$\begin{aligned} x(k) &= A(k)x(k) + B(k-1)u(k-1) + \omega(k) \\ y(k) &= g(x(k), u(k)) + v(k) \end{aligned} \quad (5)$$

in which $\omega(k)$ and $v(k)$ are the process noise and measurement noise, respectively. $A(k-1)$ and $B(k-1)$ are as follows:

$$A(k-1) = \begin{bmatrix} 1 & 0 \\ 0 & e^{-\frac{T_s}{R_1C_1}} \end{bmatrix} \quad B(k-1) = \begin{bmatrix} -\eta\frac{T_s}{C_n} \\ R_1(1 - e^{-\frac{T_s}{R_1C_1}}) \end{bmatrix}$$

Also, the state vector and the input vector are considered to be $x(k) = [SOC(k) \ U_1(k)]^T$ and $u(k) = I(k)$, respectively. Furthermore, the measurement equation is the second equation of Eq. (5). This equation is indeed (4) when considering $y(k) = U_{OC}(k)$ and $g(x(k), u(k))$ as the right-hand side of (4).

As can be seen from the final relation between the OCV and the terminal voltage of the battery, it can be concluded that there are parameters in the model whose time-varying behavior will affect the battery behavior. For example, assume the calculation of the SOC using (1). Under the time-varying behavior of the system, we cannot conclude an accurate value of the SOC due to the existence of uncertainty in the terminal current. Through the literature, some tests are defined to calculate the battery parameters as accurately as possible. For further explanation, the capacity-temperature test, the OCV-SOC temperature test, the internal resistance temperature test, and some other tests are defined in the literature to extract more accurate parameters and models for batteries. The next section describes the model of the battery proposed in this paper and introduces the parameters and the area of uncertainty in system modeling.

III. EKF for SOC estimation

The Kalman filter offers an optimal solution for filtering problems under linear and Gaussian conditions. However, SOC estimation encounters difficulties due to its nonlinear nature. Addressing nonlinear filtering problems effectively

requires a thorough description of their conditional posterior probability. Yet, providing such a detailed description involves an infinite number of parameters, rendering it impractical for real-world applications. Consequently, various suboptimal approximation methods have been proposed to tackle this challenge. An example is the EKF used to linearize nonlinear systems for optimal estimation, which is achieved by expanding the nonlinear system using the Taylor series, disregarding high-order terms, and approximating the nonlinear system with the first-order term. Subsequently, the Kalman filter method is employed to estimate the state. Let us assume that the state equation and observation equation are as follows:

$$\begin{aligned} X(k) &= AX(k-1) + BU(k) + W(k) \\ Y(k) &= g(X(k), U(k)) + V(k) \end{aligned} \quad (6)$$

in which $X(k)$ is the system state, $U(k)$ is the system input, and $Y(k)$ is the system output. Furthermore, the process and measurement noises are shown with $W(k)$ and $V(k)$. Thus, the future prediction of the system state is written as:

$$X(k|k-1) = AX(k-1|k-1) + BU(k) \quad (7)$$

in which the predicted value is shown using $X(k|k-1)$. Moreover, the optimal value of the state is shown with $X(k-1|k-1)$. In the next step, the covariance matrix is predicted as:

$$P(k|k-1) = AP(k-1|k-1)A^T + Q(k) \quad (8)$$

in which $P(k|k-1)$ is the covariance matrix. Also, the parameter $Q(k)$ is the covariance matrix of the process noise $W(k)$. An optimal estimation for the states is as follows:

$$\begin{aligned} X(k|k) &= X(k|k-1) + \\ &K(k)(Y(k) - g(X(k|k-1), U(k))) \end{aligned} \quad (9)$$

in which the matrix of $K(k)$ is the filter gain which is calculated using the following equation:

$$\begin{aligned} K_k &= P(k|k-1)H^T(k)(H(k)P(k|k-1)H^T(k) \\ &+ R(k))^{-1} \end{aligned} \quad (10)$$

$$H = \frac{\partial g}{\partial x}$$

where the matrix of $R(k)$ is the covariance matrix of measurement noise. The covariance is updated as follows:

$$P(k|k) = (I - K(k)H(k))^{-1} P(k|k-1) \quad (11)$$

Also, the measurement equation is as follows:

$$U(k) = U_{OC} - U_1(k) - R_o I(k) + V(k) \quad (12)$$

In order to reduce the complexity of the above equation, the system linear model is rewritten as follows using the Taylor expansion equations:

$$\begin{bmatrix} SOC(k) \\ U_1(k) \end{bmatrix} = \begin{bmatrix} 1 & 0 \\ 0 & 1 - \frac{T_s}{\tau} \end{bmatrix} \begin{bmatrix} SOC(k-1) \\ U_1(k-1) \end{bmatrix} + \begin{bmatrix} -\eta \frac{T_s}{C_n} \\ \frac{T_s}{C_1} \end{bmatrix} I(k-1) + \begin{bmatrix} W_1(k) \\ W_2(k) \end{bmatrix} \quad (13)$$

in which C_n is the battery capacity in the n -th cycle and $\tau = R_1 C_1$ is the time constant of the system. Based on the estimation theory, the accuracy of the estimation directly depends on the model accuracy and noise information. This can be understood from the estimation equations in different steps. Therefore, uncertainty in the dynamical model and noise information impairs the quality of SOC estimation. To solve this, as the main novelty of the paper, we present a new method to estimate the battery SOC in the presence of the mentioned uncertainties.

IV. Adaptive SOC estimation

This section is divided into two parts. The first part presents the AEKF. The second part introduces our novel approach known as RLS-AEKF.

A. SOC estimation using AEKF

A combination of the conventional EKF with an adaptive law is known as AEKF, which is given in [23-25]. The two steps of the model prediction and state correction construct the main framework of the KF theory. In the prediction step, the state values in the sampling time k are predicted. In this step, the prediction is accomplished using the system model. Therefore, obviously, the accuracy of the estimation depends on the model accuracy. In the correction step, the estimated values are updated based on the current measurement at the k -th sampling time. Apart from the model accuracy, having accurate information about the process and measurement noise is a solution key to having high-quality estimation. In the AEKF of reference [25], the adaptive law is used to update the covariance matrix over time and parallel to the EKF algorithm. Therefore, the AEKF algorithm of reference [25] uses the following update law to estimate the covariance values over time.

$$e(k) = Y(k) - g(X(k))$$

$$L(k) = \frac{1}{N} \sum_{i=k-N+1}^k e(i)e(i)^T \quad (14)$$

$$R_k = L_k + H(k)P(k|k)H(k)$$

$$Q_k = K(k)L_k K(k)^T$$

where $i = k - N + 1$ denotes the initial sample within the estimation window. The selection of the window size, denoted as N , is determined empirically to provide a degree of statistical smoothing. $e(k)$ represents the calculation of error innovation. Therefore, using Eq. (14), the noise information is updated over time. This method has some merits and drawbacks. As a merit, this method can estimate the time-varying behavior of the noise over time. On the other hand, its drawback is that it increases the computation burden. Specifically, a good estimation of noise information needs an adequately long data window (a larger value for N), which increases the computation burden. However, it seems to work acceptably for noises with slow time changes in information, as seen in the results of [25].

B. SOC estimation using RLS-AEKF

In the previous section, we discussed the common SOC background in the literature. The main gap in the SOC estimation using the aforementioned method is the use of a predefined model. The experimental results in the literature show a notable dependence between estimation and model accuracy. Consider the second row of Eq. (9), which is given as follows:

$$U_1(k) = (1 - \frac{T_s}{\tau})U_1(k-1) + (\frac{T_s}{C_1})I(k-1)$$

Defining the model parameters as

$$\theta_1 = 1 - \frac{T_s}{\tau}$$

$$\theta_2 = \frac{T_s}{C_1}$$

results in Eq. (15) as follows:

$$U_1(k) = \theta_1 U_1(k-1) + \theta_2 I(k-1) \quad (15)$$

Eq. (6) can be written as

$$\phi(k) = [U_1(k-1) \quad I(k-1)]^T$$

$$\theta = [\theta_1 \quad \theta_2]^T$$

Then, $U(k)$ can be written as:

$$U(k) = \phi^T(k)\theta(k) + \xi(k)$$

where $\xi(k)$ is set as the sampling error of the sensor at time k . Therefore, if it is possible to estimate $U_1(k), U_1(k-1)$

and $I(k-1)$, the parameters θ_1 and θ_2 can be estimated. In more detail, it leads to the estimation of R_1 and C_1 . To do that, we use the RLS method using Eq. (16) as follows:

$$\begin{aligned}\hat{\theta}(k) &= \hat{\theta}(k-1) + K(k)(y(k) - \varphi^T(k)\hat{\theta}(k-1)) \\ K(k) &= P(k-1)\varphi(k)(\lambda + \varphi^T(k)P(k-1)\varphi(k))^{-1} \\ P(k) &= (I - K(k)\varphi^T(k))P(k-1)/\lambda\end{aligned}\quad (16)$$

in which $y(k) = U_1(k)$. The parameter $\lambda \in (0, 1]$ is the forgetting factor. Furthermore, the matrix $P(k)$ is the covariance matrix of the algorithm. After identifying $\theta(k)$, the parameters of the Thevenin model can be obtained as follows:

$$\begin{aligned}C_1(k) &= \frac{T_s}{\theta_2(k)} \\ R_1(k) &= \frac{T_s}{C_1(k)(1 - \theta_1(k))}\end{aligned}$$

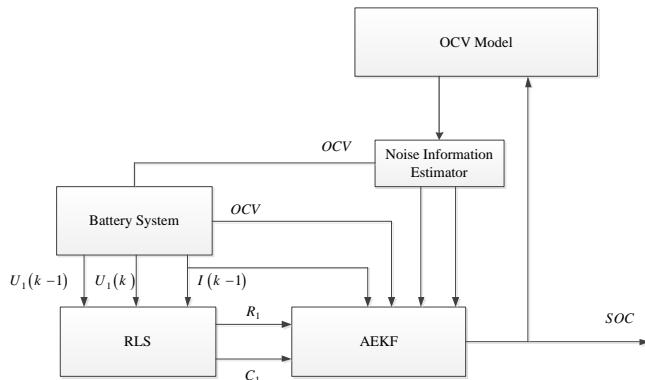


Fig. 2. The block diagram of the proposed SOC estimation

The combination of the proposed methods is presented in Fig. 2. As is seen in Fig. 2, the SOC is estimated with a composition of the RLS and adaptive EKF methods.

In more detail, the model's inner resistance and capacitor values are first estimated using the RLS identification method. Then, the values are delivered to the EKF to update the model. After that, the EKF estimates the SOC more accurately. As can be seen, the filter measurement does not depend on the other parts. Thus, the uncertainty of the measurement model also affects the estimation accuracy. To solve it, an accurate identification of the OCV curve is needed. Assuming information accuracy, we have calculated an interval for the estimation accuracy based on the OCV characteristics curve.

V. Results

The proposed method was implemented using MATLAB on a

standard laptop system equipped with an Intel Core i7 processor and 16GB of RAM. The simulation result for SOC estimation is addressed for the proposed method compared with EKF and RLS-EKF. This makes comparison possible and shows how combining adaptive estimation and system identification can improve the results.

A. Model characteristics and time-varying behavior

In the mathematical model of the battery, we assume that there is 10% uncertainty in the SOC-OCV curve, which is the total effect of some uncertainty sources listed in the literature. Therefore, if assuming the characteristic curve as follows:

$$\begin{aligned}OCV &= 1.8666SOC^5 - 5.0687SOC^4 + 5.7086SOC^3 \\ &\quad - 3.5125SOC^2 + 1.7145SOC + 3.4400\end{aligned}\quad (17)$$

then, the assumption of 10% uncertainty in the model parameters leads to Fig. (3) for the description of the characteristic curve.

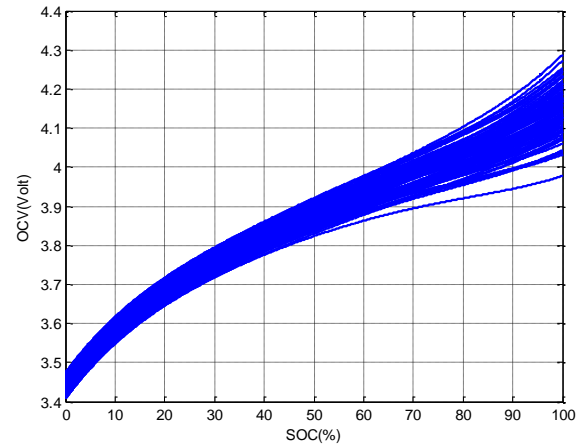


Fig. 3. Sensitivity of the battery characteristic curve with respect to 1% uncertainty in the 5-th order model parameters

As can be seen in Fig. 3, the effect of uncertainty appears to be more destructive in high voltages or high values of SOC. Similarly, the same is accomplished for the resistance and capacitor. To handle that, firstly, the nominal value of the mentioned parameters when there is no uncertainty in the values is given by:

$$\begin{aligned}R_1 &= 0.02346 - 0.10537SOC + 1.1371SOC^2 \\ &\quad - 4.55188SOC^3 + 8.26827SOC^4 - 6.93032SOC^5 \\ &\quad + 2.1787SOC^6\end{aligned}\quad (18)$$

$$\begin{aligned}C_1 &= 203.1404 + 3522.78847SOC \\ &\quad - 31392.66753SOC^2 + 122406.91269SOC^3 \\ &\quad - 227590.94382SOC^4 + 198281.56406SOC^5 \\ &\quad - 65171.90395SOC^6\end{aligned}\quad (19)$$

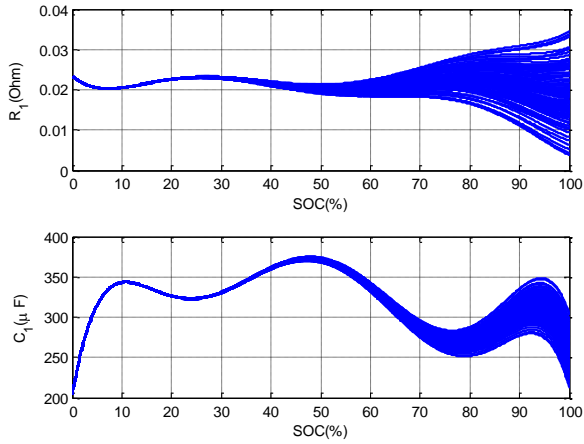


Fig. 4. The change in the resistance and capacitor values with respect to the battery SOC for 0.01% change in the polynomial curve for the calculation of the parameters

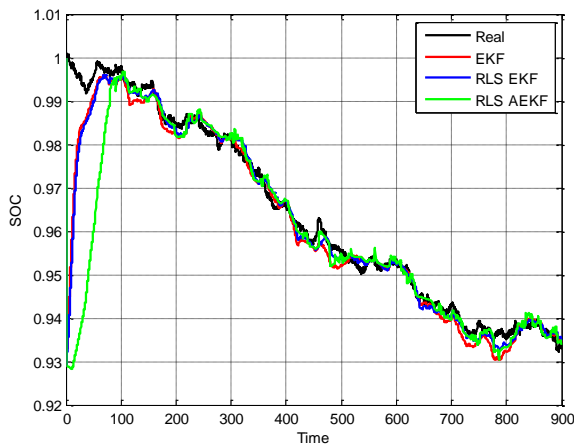


Fig. 5. The SOC estimation using the EKF, RLS-EKF, and RLS-AEKF

The above equations shall be used in simulations. However, we consider a notable uncertainty (10%) in the parameters. To have a more understandable view of the mentioned parameters and their behavior based on the operating point of the battery, we illustrate the resistance and capacitor bound in Fig. 4.

Based on the results displayed in Fig. 4, we can see that there is a notable sensitivity in the curve due to the identification error in the high values of the SOC. Therefore, it seems to be better to tune the filter robustness or adaptive behavior in the bigger values of the SOC. In other words, the identification error in small values of the SOC may not encounter the estimation with a notable error.

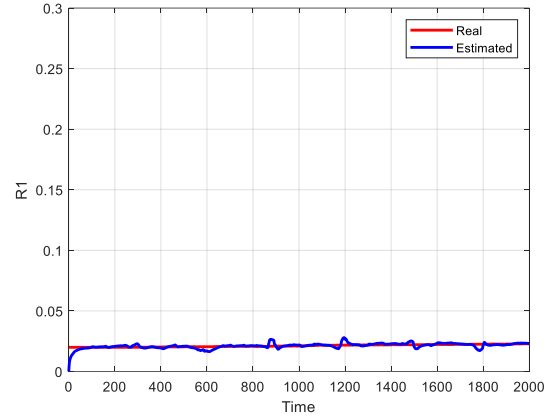


Fig. 6. The battery resistance estimation over the time using the RLS method

B. Estimation Results

This subsection presents the results for SOC estimation using RLS-AEKF, RLS-EKF [3], and EKF. It is worth noting that in the first three filters mentioned, the values of R and Q are set equal to $Q = \text{diag} [2 \times 10^{-8} \quad 1 \times 10^{-8}]$ and $R = 10^{-6}$, respectively. Finally, the simulation results for SOC estimation with the given system and estimator parameters are presented in Fig. 5. In these simulations, a 10% uncertainty is assumed in parameter identification.

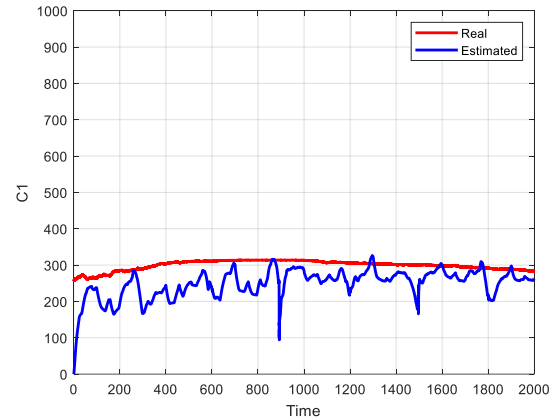


Fig. 7. The battery capacitor estimation over the time using the RLS method

Based on the results in Fig. 5, it can be concluded that the adaptive law in the estimation algorithm will remove the estimation bias. In other words, the uncertainty in the model parameters will conclude a notable bias in the estimation. The RLS estimation will update the model over time and give a more real model to the estimation algorithm (EKF). To complete the simulation results, the results of the RLS algorithm are shown below. As noted before, in the simulation, we assume that there is 10% uncertainty in the

model.

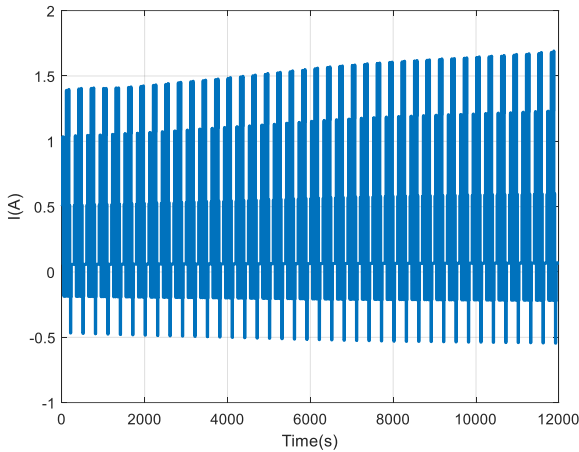


Fig. 8. The battery current during the SOC estimation

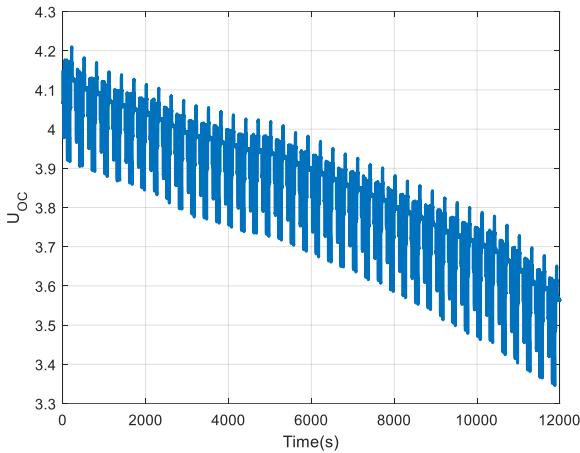


Fig. 9. The battery voltage during the SOC estimation

Figs. 6 and 7 show the parameter estimation of the algorithm. As can be seen, in the first times of the simulation, the unknown parameters are estimated, which is the main part of the paper. Furthermore, the battery terminal current and voltage are the inputs of the estimation algorithm, which is illustrated in Figs. 8 and 9, respectively. As seen in these figures, the online identification algorithm of RLS can successfully estimate the parameter values over time. Note that the ripple in the estimation value is caused by the ripples in the battery current, which is the algorithm’s input. To reduce the ripple in the identification results, we used a first-order filter as $H(s) = 1/(20s + 1)$. The introduced filter deduces the fluctuation in the output of the RLS and causes the EKF to give far better results. Moreover, the terminal voltage and current behavior is illustrated in Figs. 8 and 9. Based on the figures, there is a ripple in the output, influencing the identification quality.

Also, for more details, the figure of the estimation error is

given in Fig. 10, which proves the improvement of the SOC estimation using the online parameter estimation of RLS.

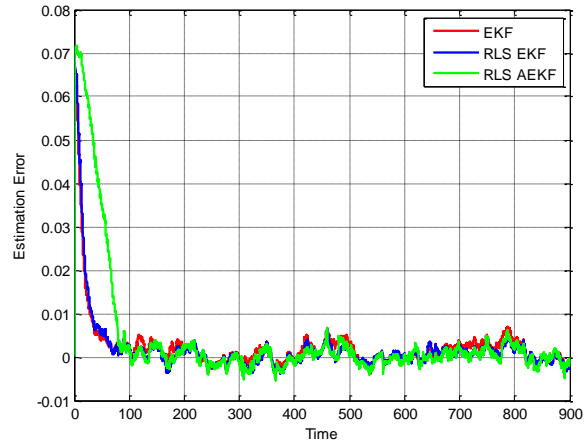


Fig. 10. The SOC estimation error using RLS-EKF and RLS-AEKF

To investigate the results more accurately, we use the root mean squared error (RMSE) criteria. Table 2 presents the RMSE associated with SOC estimation conducted by EKF, RLS-EKF [3], and RLS-AEKF. The data in Table 2 clearly demonstrate that the proposed approach surpasses alternative methods in terms of performance.

TABLE 2 RMSE OF SOC

	RMSE	Processing Time
EKF	0.033	0.8897
RLS-EKF[3]	0.0021	0.9928
RLS-AEKF	0.001	1.210

The accuracy and robustness of the proposed method are assessed using the working current profiles of the Fast Urban Driving Schedule (FUDS) and Urban Dynamometer Driving Schedule (UDDS), which are laboratory test methods used to characterize the performance of batteries, particularly for EVs. They involve applying a series of discharge and charge pulses at different magnitudes to the battery under controlled conditions. The experimental conditions are standardized with a fixed temperature of 0°C to streamline the procedures. Fig.11 illustrates the corresponding current profiles of FUDS and UDDS. Table 3 shows the estimated results of the methods under UDDS and FUDS conditions. Based on Table 3, the RMSE of the proposed method is lower than that of other methods under three working conditions.

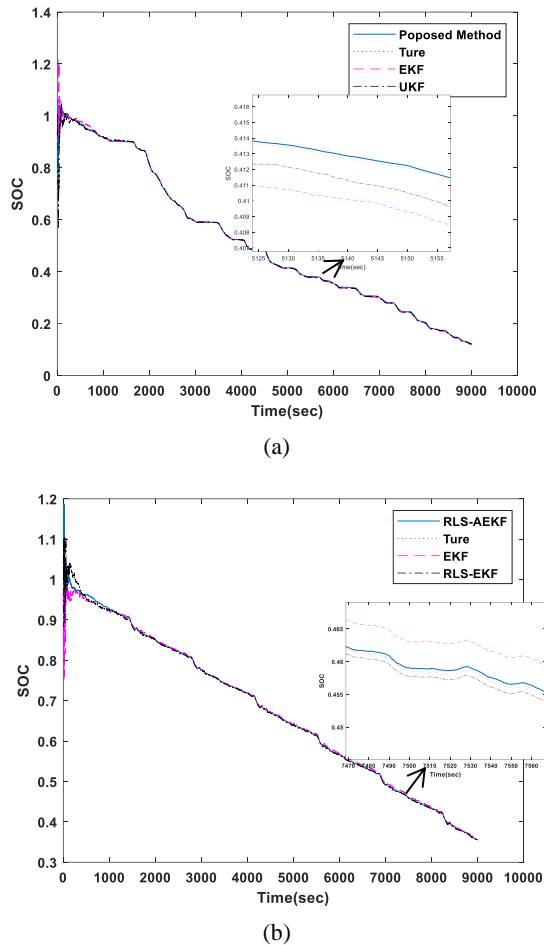


Fig.11. The RMSE of SOC at 0°C(a) UDDS (b) FUDS

TABLE 3 RMSE UNDER DIFFERENT CONDITIONS

	RLS-AEKF	RLS- EKF	EKF
UDDS	0.0087	0.011	0.018
FUDS	0.0058	0.0089	0.0108

Ultimately, the scenario where measurement noise is erroneously configured is examined. Table 4 presents a comparative analysis between the RLS-AEKF and conventional techniques, such as EKF and RLS-EKF, under FUDS and UDDS scenarios. The results indicate that the RLS-AEKF exhibits superior accuracy compared to its counterparts, highlighting its robustness in handling unknown noise statistics. The RMSE is computed over 50 Monte Carlo iterations, justifying the adaptive adjustment of process and measurement noise covariance within the proposed framework.

TABLE 4 RMSE UNDER UNKNOWN NOISE STATISTICS

	RLS-AEKF	RLS- EKF	EKF
UDDS	0.0089	0.021	0.042
FUDS	0.006	0.017	0.033

C. Monte Carlo Analysis

This sub-section investigates the problem using a Mont Carlo simulation test to investigate the effect of the parameter uncertainties on the estimation quality. To this aim, we will

run the simulation more times and then calculate the error bound of the SOC estimation error. Based on the results given in Fig. 13, we can conclude that the performance of the EKF is 2% (SOC estimation error), which is a notable error in the range of 0 to 100%. This shows the weak robustness of the filter against the parameter variation. The results for AEKF are given below. The results show that the AEKF can estimate the SOC with an accuracy of 0.4% in most cases.

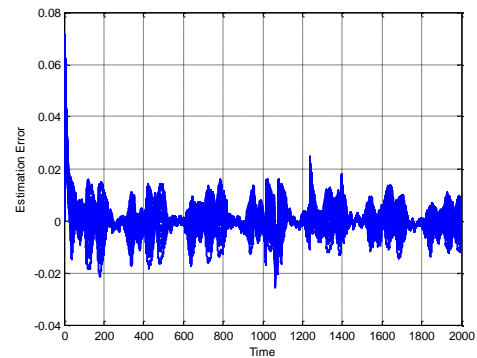


Fig. 12. Mont Carlo Simulation to investigate the effect of the parameter uncertainty on the AEKF accuracy

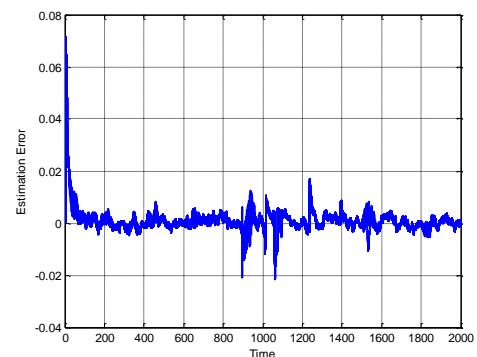


Fig. 13. Mont Carlo Simulation to investigate the effect of the parameter uncertainty on the RLS-AEKF accuracy

VI. Conclusion

This paper presented a new battery SOC estimation method in which the terminal voltage and current were measured. Due to the significance of SOC estimation in some applications, the ability of the estimation algorithm against model uncertainty is an important problem mentioned in the literature, which motivated us to find a solution to reduce the effect of uncertainty on SOC estimation. So, two algorithms were introduced to identify the deterministic uncertainty (model parameters) and stochastic parameters (noise information). To show the effect of the deterministic uncertainty, we first considered 0.02% uncertainty in the characteristics curve of the battery resistance and capacitor. In the first part of the simulation, we showed that just 0.02% uncertainty in the 5th-order polynomial causes a 10% error in

the observation of the parameters. Also, in the second part of the simulation, it was shown that the uncertainty of this parameter resulted in a notable error in SOC estimation. An online identification algorithm of RLS was introduced to identify the model's unknown parameters over time. In a parallel method, the noise information was estimated using an iterative method. Then, the overall information was given to the EKF, which was called RLS-AEKF. The results showed better accuracy of RLS-AEKF than the EKF. Finally, in the last part of the simulation, a Mont Carlo analysis was used to investigate the effect of uncertainty on the SOC estimation error bound. In case the adaptive method was used, the results of running the Mont Carlo simulation for 100 times showed the error bound of better than 0.4% in most times, i.e., about 5 times better than the non-adaptive method.

REFERENCES

- [1] P.Shrivastava, P.Naidu , S.Sharma , B.K.Panigrahi , A.Garg , “Review on technological advancement of lithium-ion battery states estimation methods for electric vehicle applications”, Journal of Energy Storage, vol.64, 2023.
- [2] G.Mohebalizadeh, H.Alipour,L.Mohammadian, M.Sabahi, “An Improved Sliding Mode Controller for DC/DC Boost Converters Used in EV Battery Chargers with Robustness against the Input Voltage Variations”, International Journal of Industrial Electronics, Control and Optimization,vol.4, no.2, pp.257-266 , 2021.
- [3] C.Ge, Y.Zheng , Y.Yu, “State of charge estimation of lithium-ion battery based on improved forgetting factor recursive least squares-extended Kalman filter joint algorithm”, Journal of Energy Storage, vol.55,2022.
- [4] K.H.Wu , M.Seyedmahmoudian, A. tojcewski, “Lithium-ion battery state of charge estimation using improved coulomb counting method with adaptive error correction” Journal of Automobile Engineering,2023.
- [5] P.Shrivastava, T.Soon , M.Y.I.B.Idris, S.Mekhilef , S. Bahari, R.S.Adnan, “Comprehensive co-estimation of lithium-ion battery state of charge, state of energy, state of power, maximum available capacity, and maximum available energy” Journal of Energy Storage,vol.6, Part B, 10 December 2022, 106049
- [6] T. Bat-Orgil, B. Dugarjav, and T. Shimizu, “Battery Module Equalizer based on State of Charge Observation derived from Overall Voltage Variation,” IEEJ J. Ind. Appl., vol. 9, no. 5, pp. 584–596, 2020.
- [7] M. Lu, X. Zhang, J. Ji, X. Xu, and Y. Zhang, “Research progress on power battery cooling technology for electric vehicles,” J. Energy Storage, vol. 27, pp. 101155, 2020.
- [8] X. Xiong, S.-L. Wang, C. Fernandez, C.-M. Yu, C.-Y. Zou, and C. Jiang, “A novel practical state of charge estimation method: an adaptive improved ampere-hour method based on composite correction factor,” Int. J. energy Res., vol. 44, no. 14, pp. 11385–11404, 2020.
- [9] B.Zine,H.Bia,A.Benmouna,M.Becherif,and M.Iqbal, “Experimentally validated coulomb counting method for Battery State-of-Charge estimation under variable current profiles,” Energies,vol.15,no.21,2022.
- [10] Y.Xiong,Y.Zhu,H.Xing,S.Lin,J.Xiao,C.Zhang, “An improved state of charge estimation of lithium-ion battery based on a dual input model,” Energy Sources, Part A,vol.45,no.1, 2023.
- [11] X. Bian , L.Liu, J.Yan, Z.Zou, R. Zhao, “An open circuit voltage-based model for state-of-health estimation of lithium-ion batteries Model development and validation,” Journal of Power Sources,vol.448,2020
- [12] A.K.Birjandi, M.F. Alavi, M.Salem, M.E.H.Assad, N. Prabakaran, “Modeling carbon dioxide emission of countries in southeast of Asia by applying artificial neural network,” International Journal of Low-Carbon Technologies,vol.17, pp.321–326, 2022.
- [13] G.Javid, D.O.Abdeslam, M. Basset, “Adaptive online state of charge estimation of EVs Lithium-Ion batteries with deep recurrent neural networks,” Energies, vol.14, 2021.
- [14] F. Yang, W. Li, C. Li, and Q. Miao, “State-of-charge estimation of lithium-ion batteries based on gated recurrent neural network,” Energy, vol. 175, pp. 66–75, 2019.
- [15] M. Talha, F. Asghar, and S. H. Kim, “A neural network-based robust online SOC and SOH estimation for sealed lead--acid batteries in renewable systems,” Arab. J. Sci. Eng., vol. 44, no. 3, pp. 1869–1881, 2019.
- [16] W. Kim, P.Y. Lee, J. Kim, K.S. Kim, “A robust state of charge estimation approach based on nonlinear battery cell model for lithium-ion batteries in electric vehicles”, IEEE Trans. Veh. Technol., vol.70, no.6, pp. 5638–5647.,2021.
- [17] Z.Huang, M. Best, J.Knowles; A.Fly, “Adaptive piecewise equivalent circuit model with SOC/SOH estimation based on extended Kalman filter,” IEEE Transactions on Energy Conversion,vol.38,no.2,2023.
- [18] T. Jarou, J. Abdouni, S. Benchikh, S. Elidrissi, and others, “The parameter update of Lithium-ion battery by the RSL algorithm for the SOC estimation under extended kalman filter (EKF-RLS),” Int. J. Eng. Appl. Phys., vol. 3, no. 2, pp. 706–719, 2023.
- [19] Y. Fang, R. Xiong, and J. Wang, “Estimation of Lithium-ion battery state of charge for electric vehicles based on dual extended Kalman filter,” Energy Procedia, vol. 152, pp. 574–579, 2018.
- [20] R. Xiong, H. He, F. Sun, X. Liu, and Z. Liu, “Model-based state of charge and peak power capability joint estimation of lithium-ion battery in plug-in hybrid electric vehicles,” J. Power Sources, vol. 229, pp. 159–169, 2013.
- [21] S. Zhang, H. Tao, K. Bi, W. Yan, and H. Ni, “SOC Estimation of Lithium-ion Battery Based on RLS-EKF for Unmanned Aerial Vehicle,” in Journal of Physics: Conference Series, pp. 12002.,2022.
- [22] M. Li, Y. Zhang, Z. Hu, Y. Zhang, and J. Zhang, “A battery SOC estimation method based on AFFRLS-EKF,” Sensors, vol. 21, no. 17, p. 5698, 2021.
- [23] C. Ge, Y. Zheng, and Y. Yu, “State of charge estimation of lithium-ion battery based on improved forgetting factor recursive least squares-extended Kalman filter joint algorithm,” J. Energy Storage, vol. 55, p. 105474, 2022.
- [24] C. Zhang, X. Li, W. Chen, G. G. Yin, J. Jiang, and others, “Robust and adaptive estimation of state of charge for lithium-ion batteries,” IEEE Trans. Ind. Electron., vol. 62, no. 8, pp. 4948–4957, 2015.
- [25] D. Sun et al., “State of charge estimation for lithium-ion battery based on an Intelligent Adaptive Extended Kalman

Filter with improved noise estimator,” *Energy*, vol. 214, p. 119025, 2021.

- [26] T. Jarou, J. Abdouni, S. Benchikh, S. Elidrissi, and others, “The parameter update of Lithium-ion battery by the RSL algorithm for the SOC estimation under extended kalman filter (EKF-RLS),” *Int. J. Eng. Appl. Phys.*, vol. 3, no. 2, pp. 706–719, 2023.
- [27] M. Li, Y. Zhang, Z. Hu, Y. Zhang, and J. Zhang, “A battery SOC estimation method based on AFFRLS-EKF,” *Sensors*, vol. 21, no. 17, pp. 5698, 2021.



Ramazan Havangi received his M.S. and Ph.D. degrees from the K.N. Toosi University of Technology, Tehran, Iran, in 2003 and 2012, respectively. He is currently an Associate Professor of control systems with the Department of Electrical and Computer Engineering, University of

Birjand, Birjand, Iran. His main research interests are inertial navigation, integrated navigation, estimation and filtering, evolutionary filtering, simultaneous localization and mapping, fuzzy, neural network, and soft computing.



Fatemeh Karimi was born in Borujerd, Iran. She received her associate degree in telecommunications, her B.Sc. degree in electronics engineering, and her M.Sc. degree in control engineering all from Islamic Azad University in 2003, 2008, and 2013, respectively. She is currently a Ph.D. candidate of control engineering at the

state-run University of Birjand. Her research interests include function fields, active power filters, multi-agents, and Kalman filters.